Impact of Surface Modification on Wakes of Two-Dimensional Cylinders

Brandon Guiseppi[1], Kaylee Rivers[2]
Tuskegee University, Tuskegee, AL 36088, USA

The understanding of the flow physics of flow separation from bluff bodies continues to be an active field of experimental and computational research. The well-known von Karman vortex street is the result of flow separation from a circular cylinder. The von Karman vortices which are shed alternately in the cylinder wake can introduce vortex-induced oscillations of the cylinder. There is a large body of research literature on understanding the shedding mechanism of the von Karman vortices and developing strategies to mitigate or control the shedding. These strategies include techniques in which the flow field is actively manipulated or influenced passively to suppress vortex shedding or change its shedding characteristics such as frequency. This research was motivated by an interesting example of a bluff body in nature is the Organ Pipe Cactus (Stenocereus thurberi) which has surface protuberances that run spanwise. The purpose of the study is to understand the wake characteristics of cylinders with surface modifications mimicking the Organ Pipe Cactus. Several 2D cylinders with sinusoidal cross-sections were studied computationally to understand the impact of surface geometry modification. Data is presented comparing the 2D cylinders with circular cross sections that have surface modification with a 2D cylinder of circular cross section.

Nomenclature
C_d = Drag coefficient
d = Diameter
Re = Reynolds Number = $U_\infty d/\nu$
U_∞ = Freestream velocity
U = Wake Profile velocity
ν = Kinematic viscosity
ρ = Fluid density

I. Introduction

The flow about bluff bodies continues to be a topic of great interest in aerodynamics, fluid mechanics, and even in areas like civil engineering and construction. A bluff body is an object that has a characteristic length along the flow that is close to the length perpendicular to the flow [1]. In aerodynamic bodies, shear stress is the main source of drag, but for bluff bodies, pressure drag is the dominating drag force [2]. Bluff body aerodynamics can describe the flow around external payloads, especially on military or rescue aircraft. Prosser and Smith present an example of a rescue helicopter, the UH-60, carrying an external cylindrical sling loaded canister to deliver emergency supplies to remote areas during natural disasters and search and rescue operations [3].

To analyze the aerodynamics of bluff bodies, a simple case of laminar flow about a circular cylinder is considered. Flow is considered laminar when Reynolds numbers, or Re, range from 0 to 2000 and the transition region is defined by Reynolds numbers between 2000 and 4000. Beyond a Re of 4000, flow is considered to be turbulent. Well-defined alternately shed vortices in the wake of a cylinder can be observed in the laminar flow regime [4].

[1] Undergraduate Student, Department of Aerospace Science Engineering, Student Member, AIAA.
[2] Undergraduate Student, Department of Aerospace Science Engineering, Student Member, AIAA.

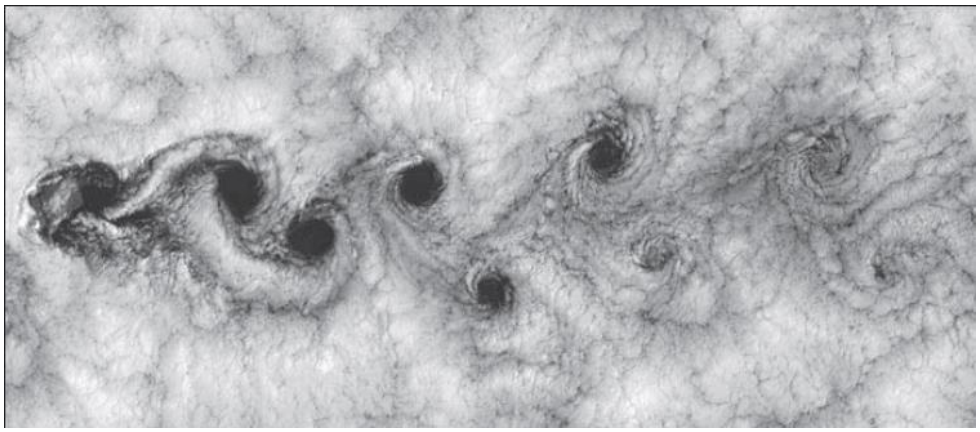

Figure 1: von Karman Vortex Street in laminar flow

These alternating vortices in low velocity aerodynamics can cause oscillations of the structure shedding the vortices. For example, the post of a stop sign or a lamp post will oscillate in a direction perpendicular to the flow direction due to von Karman vortices. These alternating vortices result in the body experiencing alternating aerodynamic forces causing structural oscillations. And while these wake patterns are natural, reducing the magnitude of these oscillations and controlling the wake patterns of bluff bodies can be very important for a variety of applications that range from aircraft and buildings.

In nature, organisms tend to adapt to their environments through natural selection. By examining the current geometry and patterns of natural organisms, such as the Organ Pipe Cactus, the topic of whether aerodynamics influenced its shape can be explored. These cacti feature ridges on the exterior that exhibit a sinusoidal-like pattern on a circular cross-section [5].

Figure 2: Organ Pipe Cactus featuring surface ridges

Because these cacti live in regions where high wind velocity is often prevalent, observing the aerodynamics around these structures may be of value.

The objective of this study was to conduct computational simulations of 2D circular cylinders with a wavy cross section and understand the wake characteristics.

II. Procedure

Using Onshape, a free, online Computer-Aided Design (CAD) software, one circular and multiple sinusoidal cylinders were created. with amplitudes of 3 mm, 6 mm, and 8 mm and a minimum diameter of 90 mm. Each was extruded to 900 mm such that 2D velocity data could be obtained with minimum end effects. The respective amplitudes were chosen to determine if their magnitude affected the drag.

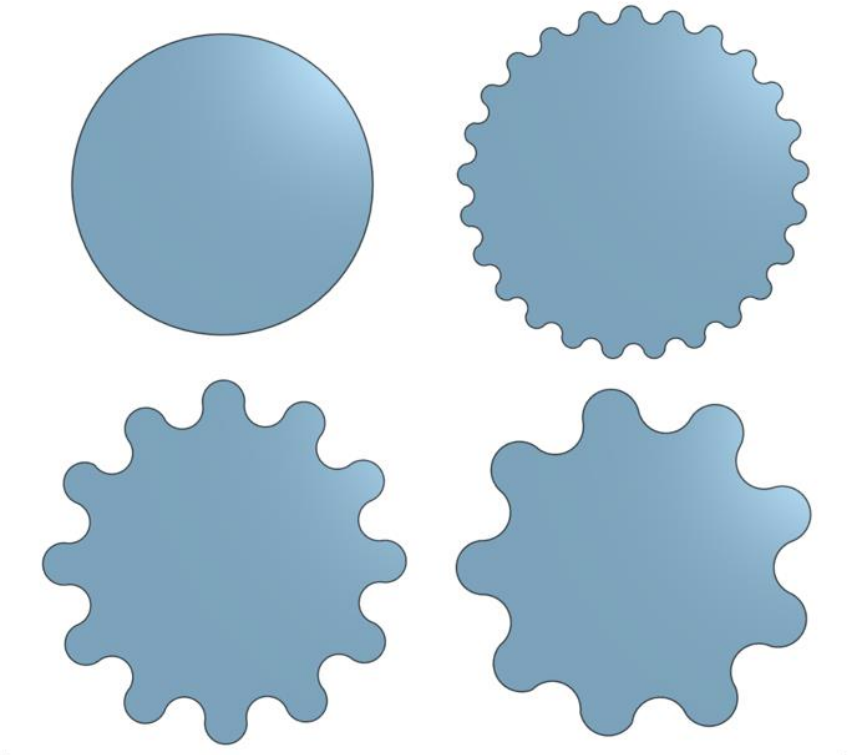

Figure 3: Cylinders modeled in Onshape - circular (top left), 3mm amplitude sinusoidal (top right), 6mm amplitude sinusoidal (bottom left), 8mm amplitude sinusoidal (bottom right)

To determine the aerodynamic effects, SimScale, a free, cloud-based Computational Fluid Dynamics (CFD) software that allows for the analysis of external and internal aerodynamics was utilized. The geometries were imported directly from Onshape to SimScale. A control volume was created around each cylinder based on diameter of the cylinder. The control volume allowed for one diameter in front of the cylinder and 8 diameters behind the cylinder. Since end effects are neglected, the depth of the control volume would be equal to the depth of the cylinder itself.

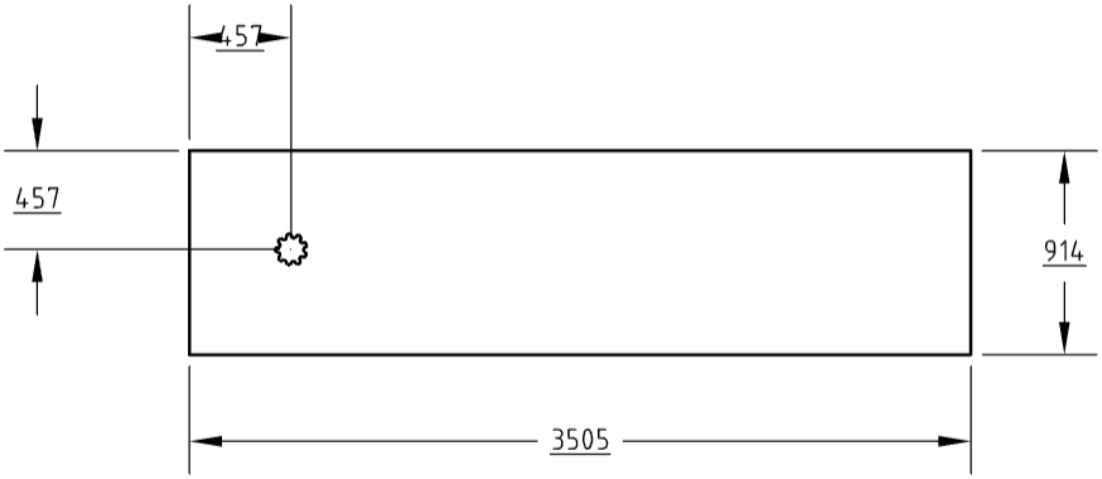

Figure 4: Dimensions of a computational volume surrounding a cylinder in SimScale (mm)

Each model was evaluated at a Reynolds number of 3000. A laminar flow simulation was run up to 750 iterations with ten 75-second intervals to track the changes in the wake over time. The boundary conditions for the simulation were as follows:

- Freestream velocity of 0.5 m/s at the inlet face
- Pressure outlet at the outlet face
- No slip walls around the cavity created by the removed cylinder
- Slip walls around the exterior walls of the control volume

Additionally, when creating the mesh, region refinements were added such that the mesh would be finer towards the immediate wake region and become coarser as the distance from the cylinder in the x-direction increased.

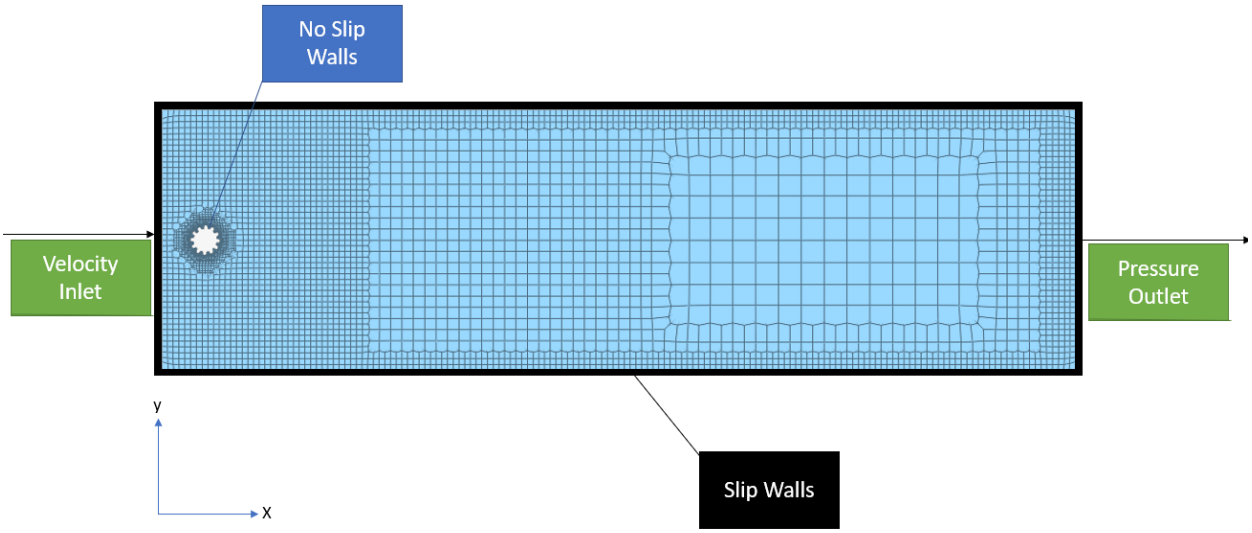

Figure 5: Boundary conditions and mesh refinements of a computational volume in SimScale

The SimScale simulation was run to 750 iterations and data was taken at every 75th iteration. After running the simulations to 750 iterations, post processing of the wake velocities was completed to analyze the velocities at five diameters behind the cylinder.

III. Results

Post processing was completed using the Paraview data visualization software. Lines of velocity normal to the flow direction were considered for each geometry at 0.55 meters, approximately five diameters, behind the trailing edge of the cylinder to obtain a velocity profile with respect to height. To ignore possible end effects of the 3-dimensional cylinder, the velocity data was taken from the center of each control volume in the z-direction to simulate a 2-dimensional cross-section. Velocity profiles of the various cylinders – circular, 3 mm, 6 mm, and 8 mm amplitude sinusoidal – were initially compared at the 750th iteration to initially compare wake profiles in Figure 6 (below).

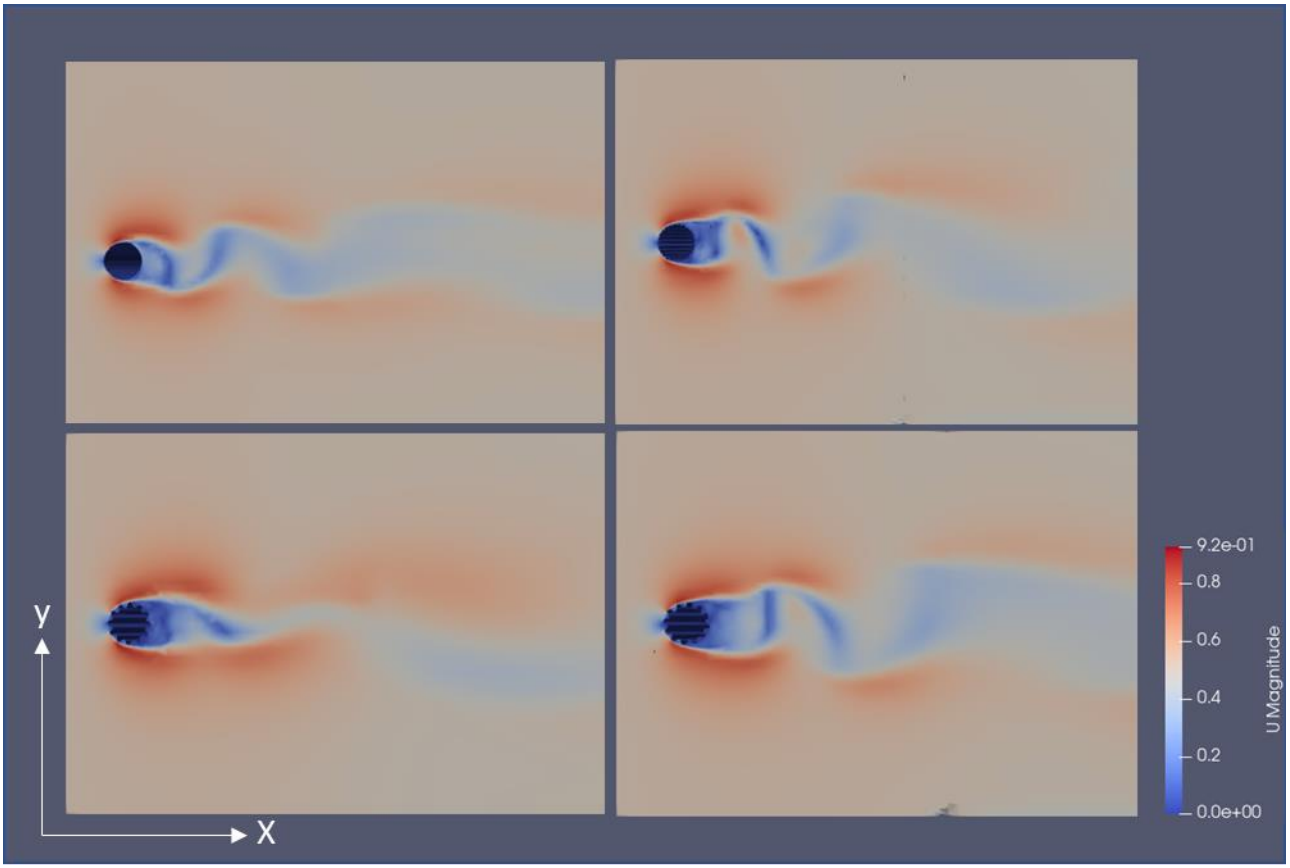

Figure 6: Cross sectional velocity contours at the 750th iteration for a) circular – top left, b) 3mm sinusoidal – top right, c) 6mm sinusoidal – bottom left and d) 8mm sinusoidal cylinders – bottom left [m/s]

The height of the velocity differences behind the actual geometry can foreshadow the drag caused by the wake profile. Initially, during the last iterations, the circular cylinder and 3mm sinusoidal cylinders have similar sized wake patterns. The 6mm sinusoidal cylinder has a much skinnier profile; the disturbance in wake velocity traveling up the y-axis is much smaller than the others. The 8mm cylinder has a much larger disruption in the wake, suggesting a larger amount of drag created.

Velocity was then averaged across all iterations to better understand the trends created by the changes in geometry. The average velocity contours were then considered to compare the wake profiles found in

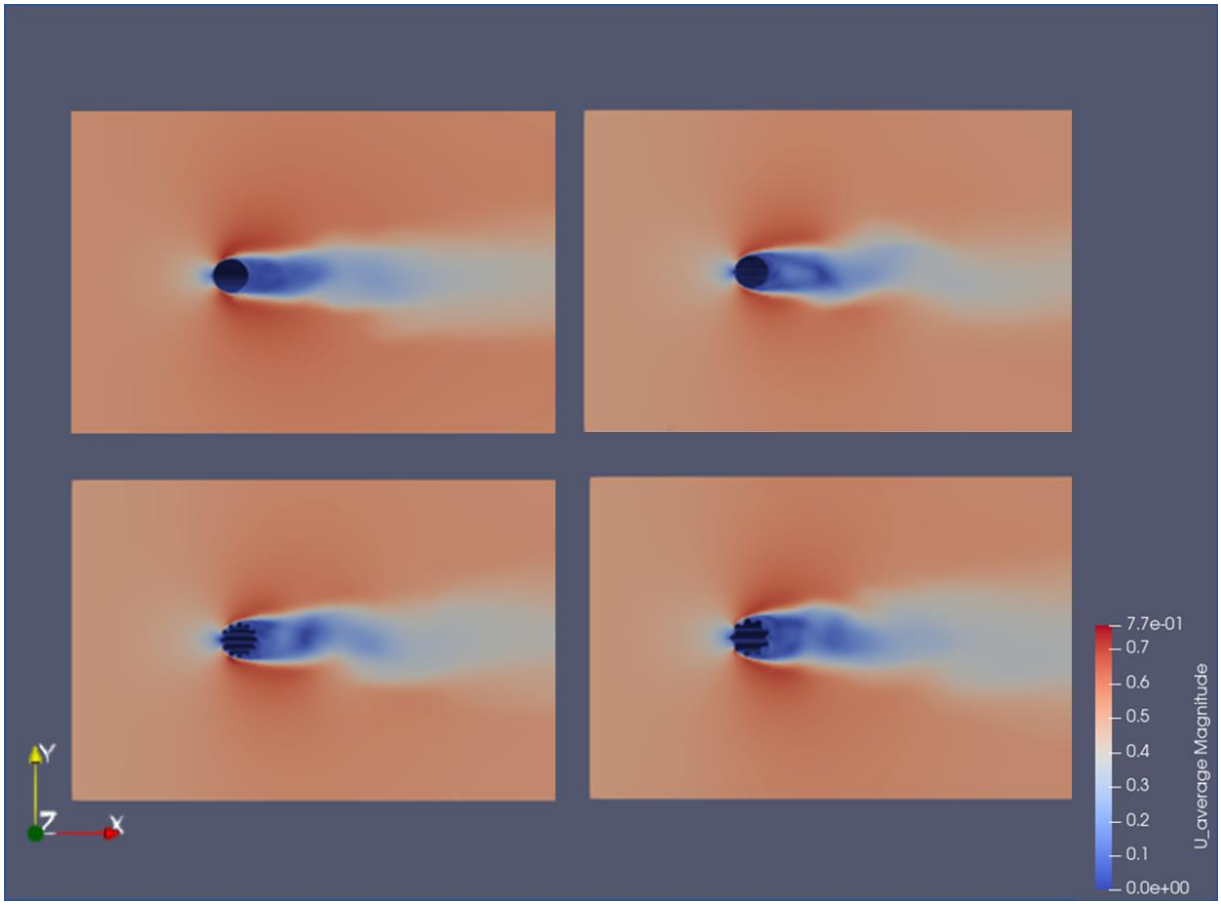

Figure 7: Average velocity contours for the circular (top left), 3mm sinusoidal (top right), 6mm sinusoidal (bottom left), and 8mm sinusoidal (bottom right) cylinders

Visually, the 8mm sinusoidal cylinder produces the largest wake disturbance over the other three cylinders. But, as it was difficult to see a sizeable change between the other cylinders' wakes, a quantitative analysis was required to track the differences in the other wakes.

Figure 8 shows average velocities plotted against the height of the control volume taken at 5 cylindrical diameters behind the trailing edge of each cylinder. Height was normalized such that the total height of the control volume would be 1, and the center of each cylinder would be at 0. Velocity was normalized by dividing the wake velocity by the inlet velocity. This would allow for the entire plot to be nondimensionalized.

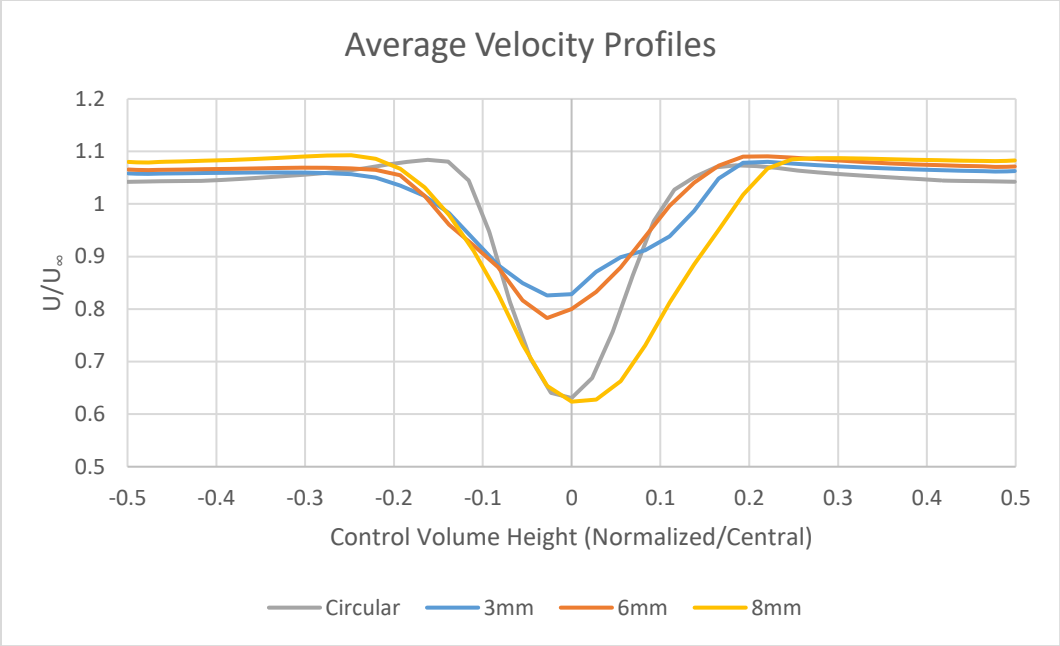

Figure 8: Velocity differences averaged over all time iterations

The two criteria that were examined in Figure 8 were the width of the area where the plot of nondimensionalized velocity is concave up, and the minimum nondimensionalized velocity. Average velocity loss is greatest for the both the circular and 8mm sinusoidal cylinder, where U/U_∞ is 0.63 for both. However, the 8mm has the larger disturbed region where the nondimensionalized velocity is less than 1 between normalized lengths of -0.15 and 0.2. The circular cylinder reaches the same maximum velocity loss, but the disturbed area is narrower – between -0.11 and 0.11 – than that of the 8mm amplitude cylinder. Both the 3mm and 6mm amplitude cylinders experience less wake velocity loss than the aforementioned shapes. The 3mm amplitude cylinder has a minimum velocity ratio of 0.82, which is higher than the 6mm amplitude cylinder at 0.78. This suggests that on average, the 3mm and 6mm sinusoidal cylinders reduce the drag from vortex shedding, while the 8mm cylinder has very little effect in reducing this drag.

Using these average velocities, the average drag was then calculated from the velocities using the equation for the drag force, $D' = \rho \int_{-h}^{h} U_2(U_1 - U_2)dy$ where $U_1 = U_\infty$ and $U_2 = U$. Drag coefficient can be obtained by the equation $c_d = \frac{D'}{q_\infty d}$ where $q_\infty = \frac{1}{2}\rho_\infty U_\infty^2$. To explore the trend between amplitude and drag coefficient, a curve fit was added to determine the existence of a correlation and to see if the data might predict where the optimal amplitude may be. This data is shown below in Figure 9.

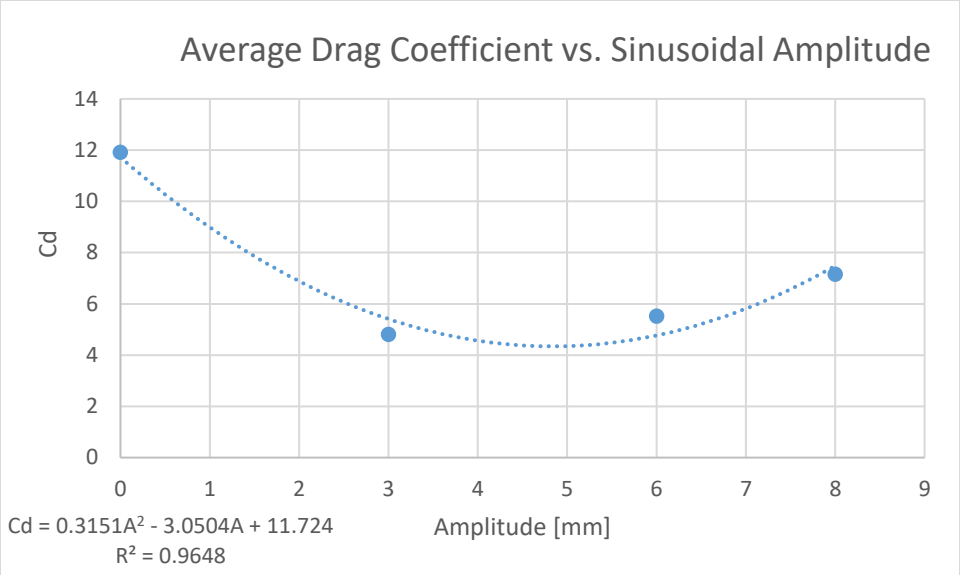

Figure 9: Average drag coefficient vs. amplitude

The above plot shows that there may exist a polynomial correlation between drag coefficient and amplitude of sinusoidal waves on the surface of the cylinder as the polynomial regression value, R^2, is greater than 90%. While this may not explain the exact relationship, it does indicate that a 4mm or 5mm datapoint should be examined in the future to see if it further reduces drag beyond the capabilities of the 3mm amplitude cylinder as it was the most effective in reducing the drag from the SimScale CFD. Table 1 shows how the average drag coefficient of circular cylinder was reduced by the sinusoidal surface modifications.

Amplitude (mm)	*Cd*	*Drag Reduction (%)*
0	11.91257	0.0
3	4.807572	59.6
6	5.51946	53.7
8	7.151622	40.0

Table 1: Average drag reduction vs. amplitude

IV. Conclusion

The results of this study reveal that modifying the surface of a cylinder with a sinusoidal shape in laminar and transition region flow can reduce the wake disturbance, and consequently, the drag as well. By adding sinusoidal ridges to circular cross sections, major drag reductions can occur in laminar and transition region flow.

Although, with only four data points the analysis is limited. While the curve fit suggests that there may be an optimal amplitude where drag coefficient is, without further testing, it cannot be verified that this is true. However, by running more analyses with more models, especially between 3mm and 6mm, and verifying these results experimentally via wind tunnel testing, the optimal amplitude for these Re may be obtained.

V. Future Plans

To verify results, 3D models of the circular and sinusoidal cylinders will be 3D printed and will be tested in a wind tunnel so that experimental data may be compared to numerical results. Other amplitudes will also be computed using CFD to get more data points for the numerical study.

VI. Acknowledgements

The research was supported by the Department of Defense, Grant # W911NF-18-1-0455.

References

[1] Konstantinidis, E. and Bouris, D. “Bluff Body Aerodynamics and Wake Control.” DOI: 10.5772/38684.

[2] Buresti, G. “Bluff Body Aerodynamics: Lecture Notes.” DOI: 10.1007/978-3-030-94195-6_20.

[3] Prosser, D. T. and Smith, M. J. “Three-Dimensional Bluff Body Aerodynamics and Its Importance for Helicopter Sling Loads.” URL: https://fun3d.larc.nasa.gov/papers/prosser_smith_erf_2014.pdf

[4] Anderson Jr., John D., *Fundamentals of Aerodynamics*, 6th ed., New York, New York, 2017, pp. 137-142, 298.

[5] Talley, S. and Mungal, G. “Flow around cactus-shaped cylinders,” *Center for Turbulence Research Annual Research Briefs 2002*, pp. 363-376. URL: https://web.stanford.edu/group/ctr/ResBriefs02/talley.pdf.